

Jian Sun^a (Jian.Sun86@du.edu), Mohammad H. Mahoor^b
(mohammad.mahoor@du.edu)

^a Department Of Computer Science, University of Denver, 2155 E Wesley Ave, Denver, Colorado, 80210, United States of America

^b Department Of Electrical and Computer Engineering, University of Denver, 2155 E Wesley Ave, Denver, Colorado, 80210, United States of America

Corresponding Author:

Mohammad H. Mahoor

Department Of Electrical and Computer Engineering, University of Denver, 2155 E Wesley Ave, Denver, Colorado, 80210, United States of America

Tel: +1 (303) 871-3745

Email: mohammad.mahoor@du.edu

Author contributions Jian Sun: Conceptualization, Methodology, Software, Validation, Formal analysis, Investigation, Data Curation, Writing - Original Draft, Writing - Review & Editing, Visualization, Project Administration. Mohammad H. Mahoor: Resources, Writing - Review & Editing, Supervision, Project Administration.

Contrastive Learning-based Video Quality Assessment-jointed Video Vision Transformer for Video Recognition

Jian Sun¹ and Mohammad H. Mahoor^{2*}

¹Department Of Computer Science, University of Denver, 2155 E Wesley Ave, Denver, 80210, CO, United States of America.

^{2*}Department Of Electrical and Computer Engineering, University of Denver, 2155 E Wesley Ave, Denver, 80210, CO, United States of America.

*Corresponding author(s). E-mail(s): mohammad.mahoor@du.edu;
Contributing authors: Jian.Sun86@du.edu;

Abstract

Video quality significantly affects video classification. We found this problem when we classified Mild Cognitive Impairment well from clear videos, but worse from blurred ones. From then, we realized that referring to Video Quality Assessment (VQA) may improve video classification. This paper proposed Self-Supervised Learning-based Video Vision Transformer combined with No-reference VQA for video classification (SSL-V3) to fulfill the goal. SSL-V3 leverages Combined-SSL mechanism to join VQA into video classification and address the label shortage of VQA, which commonly occurs in video datasets, making it impossible to provide an accurate Video Quality Score. In brief, Combined-SSL takes video quality score as a factor to directly tune the feature map of the video classification. Then, the score, as an intersected point, links VQA and classification, using the supervised classification task to tune the parameters of VQA. SSL-V3 achieved robust experimental results on two datasets. For example, it reached an accuracy of 94.87% on some interview videos in the I-CONNECT (a facial video-involved healthcare dataset), verifying SSL-V3's effectiveness.

Keywords: Contrastive Learning, Data Imbalance, NR-VQA, Self-Supervised Learning, Video Classification, ViViT

1 Introduction

Video Classification is a critical research problem within Computer Vision, affected by several factors such as video quality [1]. The problem also exists in other domains, especially healthcare research and applications, where detects mild cognitive impairment (MCI) in older adults through video interviews [2, 3]. For example, a Video Vision Transformer model (ViViT) achieved better predictions on high-quality videos than blurred ones (see Fig. 5 as examples), which adversely affected the results. The ViViT model correctly predicted 20 out of 20 subjects (100% accuracy) from subjects with high-quality videos, while only achieving 58.33% accuracy (5 out of 12) in subjects with poor-quality videos.

Given that video classification results can be significantly influenced by video quality, this article explores the integration of video quality assessment into video classification tasks to enhance model performance. Specifically, we investigate methods to incorporate video quality scores as a contributing factor in classification.

To achieve this objective, we first propose a mechanism that allows video classification models to leverage video quality scores effectively. A potential approach involves the development of a loss function that integrates video quality scores to guide model optimization. However, the success of this approach hinges on the availability of precise video quality scores. Consequently, the second key task is to develop accurate methods for calculating these scores, ensuring their reliability for downstream classification tasks.

Most current video datasets lack ground truth video quality scores. No-Reference Video Quality Assessment (NR-VQA) can address this critical limitation [4, 5]. However, NR-VQA predominantly relies on Mean Opinion Scores (MOS) to compute loss values [6, 7]. The process of collecting MOS is labor-intensive, costly, and time-consuming, which significantly constrains the potential for precise video quality score prediction via traditional NR-VQA approaches.

In this paper, we propose a method based on Self Supervised Learning (SSL) [8] to address the problem of lacking video quality scores/labels. SSL benefits many video tasks such as Video Segmentation [9]. Specifically, we apply the chain rule during back-propagation to simultaneously address three critical issues: 1) fusing video quality score into video classification, 2) quality score label shortage, and 3) calculating accurate video quality score). Ultimately, we create a Combined-SSL mechanism that integrates pretext tasks, downstream tasks, and Contrastive Learning.

Video quality scores are weight factors to calibrate the learned classification features through the Tune-CLS module. The video quality score emerges as a pivotal parameter at the intersection of Video Quality Assessment (VQA) and classification tasks. The chain rule ensures model optimization of VQA alongside video quality score estimation via back-propagation. Consequently, a precise video quality score enables more objective and accurate predictions, establishing a cyclical reciprocal relationship where regression supports classification and classification supports regression. This approach directly addresses our research’s video quality score label scarcity challenge.

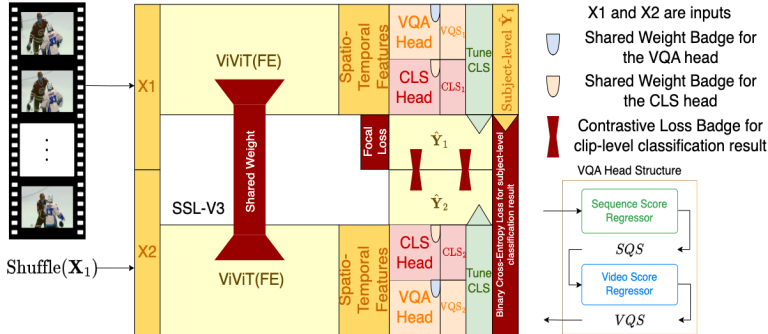


Fig. 1: The structure of the new proposed SSL-V3. In the upper branch, ViViT(FE) loads \mathbf{X}_1 and extracts Spatio-Temporal features f_{S_1} . The VQA head and classification (CLS) head then process f_{S_1} to compute VQS_1 and CLS_1 , respectively - output features from each head. VQA head contains Sequence Score Regressor and Video Score Regressor, while CLS head is Multi-branch Classifier. The Tune-CLS module updates CLS_1 using VQS_1 to produce the prediction score \hat{Y}_1 . Simultaneously, the lower branch follows the same procedure to generate f_{S_2} , VQS_2 , CLS_2 , and \hat{Y}_2 .

Furthermore, to enhance feature distinguishability, Combined-SSL employs Contrastive Learning by creating a parallel identical branch with shared weights. Fundamentally, Combined-SSL comprises the Tune-CLS module, integrating pretext tasks and downstream tasks within a contrastive structure.

To derive objective and precise video quality scores, we designed a cascading VQA regressor head featuring two components: the Sequence Score Regressor and the Video Score Regressor. This hierarchical approach enables progressive quality score regression from individual sequences to the entire video clip.

We developed SSL-V3 (**SSL**-based ViViT Combined with NR-VQA for Video Classification), a model architecture comprising the ViViT backbone with the Factorised Encoder (FE) [10], a classification head, the proposed Combined-SSL mechanism, and the VQA head. The ViViT (FE) excels at capturing Spatio-Temporal features, while the MC (Multi-branch Classifier) module from MC-ViViT [2] serves as the classification head.

To ensure optimal model convergence, we proposed a new loss function, which simultaneously optimizes SSL-V3 at both batch and subject levels.

We validated SSL-V3 on the I-CONNECT dataset and conducted an additional experiment on the violence detection dataset to demonstrate the model’s generalizability. The experimental results substantively verify that incorporating video quality scores significantly enhances the deep learning model’s video classification capabilities, confirming Combined-SSL as a robust methodological approach.

In summary, the primary objective of this study is to improve video classification performance by integrating NR-VQA using a self-supervised mechanism (SSL-V3). All contributions of this paper are as follows:

- We propose the Combined-SSL framework, which is a theoretical contribution that leverages the reciprocal relationship between the VQA task and Contrastive Learning to classify videos objectively.

- We develop the SSL-V3 model to implement the Combined-SSL mechanism.
- We present a hierarchical VQA head designed to regress video quality score, incorporating Sequence Score Regressor and Video Score Regressor modules.
- We design a new Loss function to address class imbalance issues and control training at batch and subject levels.
- Our experimental results on two wild datasets using SSL-V3 demonstrate that integrating VQA benefits video classification and SSL-V3 is capable of practical application.

The rest of this paper includes these contents: Section 2 reviews the related works on VQA and SSL. Section 3 illustrates the SSL-V3 model and CBS Loss. Section 4 discusses the datasets and experiment setup. Section 5 presents an analysis of the SSL-V3 model, highlights the limitations of the study, and suggests future work. Finally, Section 6 concludes the paper.

2 Related Work

This section first reviews approaches to regress video quality scores. Subsequently, it discusses the drawbacks of optimizing video quality scores in the current Self-Supervised Learning algorithms.

2.1 Video Quality Assessment (VQA)

VQA [11, 12] is categorized into three main types: Full-Reference, Reduced-Reference, and No-Reference (NR) models [13], based on the availability of reference information. NR-VQA is the unsupervised learning model, making it more practical for real-world applications where labels are scarce [13, 14]. Thus, this paper focuses on NR-VQA, drawing inspiration from the following ideas:

Weight averaging calculates the video quality score from the Sequence Quality Score [15]. Kim *et al.* [15] designed a path weight estimator to generate a learnable patch weight. However, they derived the video quality score from the patch quality score directly.

In VQA, Past frames influence the current frame, and the current frame also affects future frames [16]. Sun *et al.* [16] implemented 1D Convolutional operations on temporal features to compute the temporal-motion effect and temporal-hysteresis effect. However, it is the frame-level effect.

In contrast to previous works, this paper studies the temporal effect at the sequence level and hierarchically regresses video quality scores from sequential features to sequence scores and finally to video scores. Additionally, this paper applies ViViT to capture Spatio-Temporal features for the VQA task, as the Transformer model captures the Spatio-Temporal features more efficiently in a single branch [2, 4] compared to CNNs [17].

2.2 Self-Supervised Learning (SSL)

SSL includes two typical approaches: Pretext Task and Contrastive Learning. SSL demonstrates its capability in many video-related tasks such as Behavioral Key-point Discovery [18], prognostics and health management [19], Video Anomaly Detection [20], and even VQA [21].

2.2.1 The Problem of Directly Applying SSL to do VQA on videos

This paper aims to improve the video classification by referring to VQA, and performing both tasks together. The biggest concern is missing VQA labels, making it impossible to fine-tune the regression head with supervision. Labeling these videos is tedious and time-consuming.

Pretext Task and Contrastive Learning may offer solutions. The structure of pretext tasks combined with downstream tasks can perform multi-task learning (video classification and video quality score estimation simultaneously), by placing two multi-layer perceptron heads in parallel. However, selecting the ideal pretext tasks to extract the desired representations is challenging and training pretext tasks before downstream tasks is time-consuming. The lack of video-quality labels further complicates this approach.

Using a contrastive structure or mean teacher [22, 23] can facilitate regression without labels. Since Contrastive Learning drops the pretext part and focuses solely on the downstream task, it is more efficient. Examples include SimCLR [24] and MoCo v1 [25], v2 [26], and v3 [27], which have simple end-to-end structure. However, Contrastive Learning requires data augmentation or video distortion, which can alter the original video quality. To use VQA alongside classification, maintaining the original input is crucial to avoid residuals. Dropping data augmentation, however, hinders the model’s generalization. Thus, singly applying either Pretext Task or Contrastive Learning is unsuitable for NR-VQA in our case, but both offer valuable insights.

The Pretext Task approach shows that pretext and downstream tasks share the same backbone, and the pretext task benefits the downstream task. Conversely, downstream tasks can also aid the pretext task (Section 3.4).

Contrastive Learning relies on a consistency strategy, connecting representations from different branches and calculating cosine similarity to measure the disparity between representations [5, 28, 29]. The closer the feature pairs are, the higher the similarity score, akin to the inverse logic of Energy in EBGAN [30]. This strategy can help supervise the classification task (Section 3.4).

The Transformer model can serve as the backbone of SSL and analyze videos effectively. For instance, Chen *et al.* [27] created MoCo v3 using ViT as the backbone, and Feichtenhofer *et al.* [31] validated that MoCo can analyze videos. Therefore, we chose ViViT as the backbone.

3 SSL-based ViViT Combined with NR-VQA for Video Classification (SSL-V3)

The proposed SSL-V3 contains two branches: the upper branch, which includes five modules-ViViT(FE), classification head, VQA head, Tune-CLS, and Combined-SSL, and the bottom branch, which performs contrastive learning. Both branches share the same structure and weights. The input \mathbf{X}_1 contain augmented video clips, the input \mathbf{X}_2 is the shuffled \mathbf{X}_1 (resort clips within the mini-batch). Fig. 1 illustrates the model architecture.

In particular, the Combined-SSL module, incorporating Tune-CLS and contrastive learning, refines the prediction scores by integrating VQA and addressing missing labels. Finally, the new loss function ensures the convergence of SSL-V3. The following subsections are the details.

3.1 ViViT backbone

ViViT [10] is a powerful generalized model, which serves as backbone for VQA as well [14, 32]. Thereby, we use ViViT with Factorised Encoder(FE) as the backbone of VQA and classification, which forces ViViT to mine various features to meet different needs. In addition, Multi-branch Classifier (MC) [2] acts as the classification head [33–35].

ViViT takes the Tubelet Embedding to split an input video clip $[T, H, W, 3]$ into non-overlapped small cubes, where T is the frame numbers, H and W are the height and the width of each frame, and 3 represents the RGB channels. The cube size is $[t, h, w, 3]$, where t , h , and w are the size of the corresponding temporal, height, and width dimensions. $n_t = \lfloor \frac{T}{t} \rfloor^1$, $n_h = \lfloor \frac{H}{h} \rfloor$, and $n_w = \lfloor \frac{W}{w} \rfloor$ denote the token number of the respective temporal, height, and width dimensions.

In the upper branch, ViViT(FE) loads \mathbf{X}_1 and learns the Sequence-level Spatio-Temporal feature f_{S_1} with the shape of $[\text{bs}, n_t+1, \text{d}]$, where bs is the batch size. n_t+1 represents n_t sequences of one clip and 1 class token, d is the feature dimension of each sequence, $\text{d} = 192$. The bottom branch follows the same process.

3.2 VQA head

3.2.1 Sequence Score Regressor (SSR)

Inspired by patch-wise quality regression network and patch-wise weight estimate network [36] and DeepVR-VQA [15], we change the structure and design Sequence Score Regressor. Fig. 2 presents its structure.

The Sequence Score Regressor adopts Sequence-level Spatio-Temporal feature f_{S_1} as the input and has two channels: Sequence Feature Processor and Sequence Weight Estimate Network. The Sequence Feature Processor drops f_{S_1} 's class token and reshapes the tensor to $[\text{bs}, n_t, \text{d}, 1]$. The Sequence Weight Estimate Network aims to generate learnable weight \tilde{w}_{f_i} for $f_{S_{1,i}}$, $i \in [1, n_t]$. It contains one FC layer and one Softmax operation. It also removes f_{S_1} 's class token and reshapes the output \tilde{w}_f to

¹ $\lfloor \cdot / \cdot \rfloor$ denotes the operation of obtaining the largest integer not greater than \cdot / \cdot .

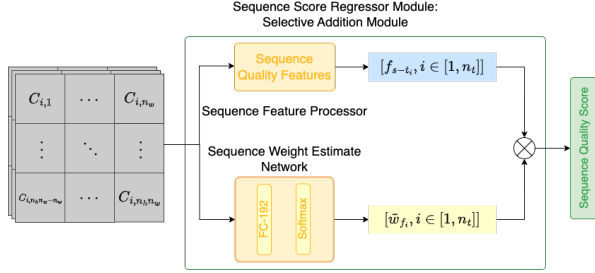


Fig. 2: The structure of Sequence Score Regressor. It has two channels. The first one, Sequence Feature Processor, is to drop the z_{cls1} and reshape f_{S_1} from $[bs, n_t, d]$ to $[bs, n_t, d, 1]$. The other one, Sequence Weight Estimate Network, is to generate weights, \tilde{w}_f for corresponding f_{S_1} . Finally, it conducts weighted sum operation to get SQS_1 . $C_{i,j}$ is the j^{th} cube from the i^{th} sequence in a certain clip.

$[bs, n_t, 1, d]$. Softmax makes \tilde{w}_f more distinguishable and restricts its range between 0 and 1.

The product and sum of $f_{S_{1,i}}$ and \tilde{w}_{f_i} equals to the i^{th} sequence quality score (SQS), $SQS_{1,i}$ (Eq. (1)).

$$SQS_{1,i} = \sum_{j=1}^{n_h n_w} \tilde{w}_{f_i} f_{S_{1,i}} \quad (1)$$

A learnable weight vector enables the model to assign smaller weights to the features in a sequence that weakly influences $SQS_{1,i}$ but allocates bigger weights to ones that significantly affect $SQS_{1,i}$. Hence, the model focuses more on valuable Spatio-Temporal features. SQS_2 comes from the same way in the bottom branch.

3.2.2 Video Score Regressor (VSR)

The work presented in [16] stated that the quality of the past frames affects the current one (temporal-motion effect), while the current frame impacts the next frames (temporal-hysteresis effect). Also, Feng *et al.* [32] and Imani *et al.* [14] discuss that regression methods for 2D patches can apply to cubic patches. Therefore, we design Video Score Regressor (VSR) based on Tang *et al.* [36].

Fig. 3 shows that the three-channel VSR accepts the sequence quality score vector SQS_1 as the input, where $SQS_1 = (SQS_{1,1}, SQS_{1,2}, \dots, SQS_{1,n_t})$. In the meanwhile, let $S = (S_1, S_2, \dots, S_{n_t})$ denote all the sequences. Then, the upper channel calculates the temporal-motion effect score s_1 , the middle one regresses a comprehensive score over SQS_1 , which is s_2 , and the bottom one computes the temporal-hysteresis effect score s_3 .

s_1 is the weighted-sum value of SQS_1 , and \hat{m} is the weight vector that the Video Score Regressor learns in the upper channel. We use a 1D convolutional operation (Conv1D) on SQS_1 followed by Softmax to compute \hat{m} , where $\hat{m} = (\hat{m}_1, \hat{m}_2, \dots, \hat{m}_{n_t})$. \hat{m}_i represents the motion effect of the past ks sequences on S_i ($i \in [1, n_t]$). Eq. (2) summarizes the entire process.

$$\begin{aligned} \hat{m} &= \text{Softmax}(\text{Conv1D}(SQS_1, k_1)) \\ s_1 &= \hat{m} * SQS_1 \end{aligned} \quad (2)$$

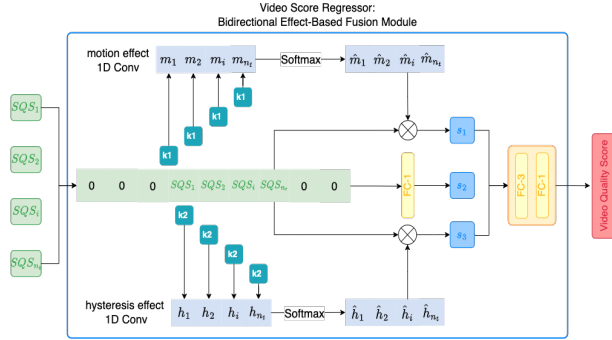


Fig. 3: The structure of VSR. It has three channels. The central one is the SQS_1 , denoted by s_2 . The upper one does 1-D convolutional operation on SQS_1 and captures the temporal motion effect, m_j , of the $SQS_{1,j}$. Then, we deploy the Softmax operation to normalize the weight vector m and output \hat{m} . Multiplying SQS_1 and \hat{m} returns the temporal motion effect score s_1 . Following the same pattern, we get the normalized temporal hysteresis effect \hat{h} and the temporal hysteresis effect score s_3 . Finally, the Temporal Memory-Based Fusion Module generates VQS_1 by concatenating s_1 , s_2 , and s_3 and loading them into a two-layers FC module.

where k_1 is the convolutional kernel with size of $[1, 1, ks]$ ($ks = 4$). We conduct zero padding before SQS_1 to ensure its dimension matches the kernel's. $*$ denotes the weighted-sum operation. This function is also applicable to s_3 , the temporal-hysteresis effect score, which measures the effect of the current sequence S_i on the later sequence S_{i+ks} .

To avoid losing important information due to simple global average pooling, we implement one FC layer on SQS_1 to regress the comprehensive score S_2 . This is the novel part of the original module. The last step is to feed the two FC layers the concatenated s_1 , s_2 , and s_3 to predict the overall video quality score (VQS), VQS_1 . The bottom branch follows the same pattern to calculate VQS_2 . This structure helps the model to conclude clip-level video scores stereoscopically and objectively.

Generally, the VQA head contains SSR and VSR modules.

3.3 Tune-CLS: Tuning the classification task using video quality score

Objectively, predictions of high-quality clips are more reliable than those of low-quality clips, motivating to assign greater confidence to the CLS_1 's results. To fulfill this target, Tune-CLS scales the maximum feature value of CLS_1 by VQS_1 prior to applying Softmax (Eq. (3)). Tune-CLS amplifies CLS_1 's maximum value and protrudes it during the Softmax operation. Conversely, for low- VQS_1 clips, the results are less trustworthy, Tune-CLS suppresses its maximum feature value.

$$\begin{aligned}
 CLS_1 &= [CLS_{1,1}, CLS_{1,2}, \dots, CLS_{1,k}] \\
 CLS_{1,i_{max}} &= CLS_{1,i_{max}} \times VQS_1 \\
 \hat{Y}_1 &= \text{argmax}(\text{Softmax}(CLS_1))
 \end{aligned} \tag{3}$$

where k is the category number, i_{max} is the index of CLS_1 's maximum value, and \hat{Y}_1 is the final prediction. Bottom branch updates CLS_2 by VQS_2 and compute \hat{Y}_2 by Tune-CLS too. In summary, the Tune-CLS module is like a no-addition involved FC layer. It revises the learned features.

3.4 Combined-SSL: Conjugate between Regression and Classification

VQA regression task misses ground truth label, which is the primary challenge of this work (i.e., we do not have any labels for the video qualities, whether the quality is low, high, etc). Combined-SSL, a novel self-supervised learning (SSL) mechanism, handles this problem by integrating the Tune-CLS module and Contrastive Learning.

The Tune-CLS module incorporates video quality scores (VQS) into the classification task, enabling the simultaneous training of regression and classification objectives. Meanwhile, Contrastive Learning strengthens the bottom branch, enhancing both VQA and classification tasks. In this framework, VQA serves as the pretext task, while classification acts as the downstream task. The SSL is only applied to the portion that deals with video quality but not the class label (NC/MCI). This dual-task learning strategy, combined with Contrastive Learning, underpins the design of Combined-SSL.

3.4.1 Combined-SSL Inspired by Chain Rule

Let Θ_{CLS} represents all the parameters of classification. VQS_1 involves in classification and belongs to Θ_{CLS} . Eq. (4) defines the gradient of VQS_1 , ∇_{VQS_1} . Notably, VQS_1 intersects both VQA and classification tasks so that the chain rule facilitates the computation and optimization of VQA parameters.

VQS_1 serves as a bridge between the pretext VQA task and the downstream classification task, benefiting in optimizing the gradients of VQA's parameters without relying on labels. Specifically, let $\Theta_{VQA} = \{\theta_{VQA_1}, \theta_{VQA_2}, \dots, \theta_{VQA_i}, \dots\}$ represent the parameters of the VQA task. For a given parameter θ_{VQA_i} , its gradient $\nabla_{\theta_{VQA_i}}$ is derived from Eq. (5).

$$\nabla_{VQS} = \frac{\partial \text{Softmax}(CLS_1)}{\partial VQS_1} \quad (4)$$

$$\nabla_{\theta_{VQA_i}} = \frac{\partial \text{Softmax}(CLS_1)}{\partial VQS_1} \times \frac{\partial VQS_1}{\partial \theta_{VQA_i}} \quad (5)$$

This mechanism effectively updates VQA parameters in a self-supervised setting, and allows the downstream classification task to influence and optimize the pretext VQA task. As a result, the SSL-V3 framework trains both tasks concurrently, leveraging the synergies between them.

3.4.2 The Integration of Contrastive Learning

To enhance feature differentiation and improve accuracy, we incorporate a parallel contrastive structure as the bottom branch, sharing the same weights and structure with the upper branch.

One key advantage is to generate new labels. When the input pair from the two branches belongs to the same category, the pair is assigned a label of 1 (positive pair); otherwise, the label is 0 (negative pair). The contrastive loss, defined in Eq. (8), quantifies the similarity between the outputs of the two branches. Additionally, these new labels introduce a supplementary supervised learning component, further fine-tuning both tasks.

In summary, Combined-SSL integrates pretext tasks, downstream tasks, and Contrastive Learning, creating a unified framework that enhances feature distinction for both tasks. It roots in the chain rule, and seamlessly optimizes parameters across integrated tasks.

3.5 Combined Batch- and Subject-level (CBS) Loss

The SSL-V3 model employs batch- and subject-level loss functions (See Eq. (6)). The batch-level loss comprises Focal Loss and Contrastive loss. The subject-level loss is a Binary Cross Entropy (BCE) loss. Although this paper focuses on binary classification, the method can be extended to multi-class classification.

$$\begin{aligned} L_{CBS} &= \text{Batch-level Loss} \\ &+ I * 0.5 * \text{Subject-level Loss} \end{aligned} \quad (6)$$

$$= FL + 0.5 * CL + I * 0.5 * BCE$$

$$I = \begin{cases} 1 & \text{if last batch} \\ 0 & \text{otherwise} \end{cases} \quad (7)$$

where FL denotes Focal Loss, while CL represents Contrastive loss. I is an indicator that signifies whether it meets the last batch.

To be specific, If the dataset has inter- and intra-class imbalanced issues [2], Focal Loss solves inter-class imbalanced issues, while Contrastive loss (See Eq. (8)) addresses intra-class imbalanced ones.

$$\begin{aligned} CL(\theta_{CLS}, (M, CLS_1, CLS_2)) &= \frac{1}{2n} \sum_{i=1}^n M * D_{\theta_{CLS}}^2 \\ &+ (1 - M) \max(m - D_{\theta_{CLS}}, 0)^2 \\ D_{\theta_{CLS}}(CLS_1, CLS_2) &= ||CLS_1 - CLS_2||_2 \\ &= \left(\sum_{j=1}^P (CLS_1^j - CLS_2^j)^2 \right)^{1/2} \end{aligned} \quad (8)$$

where θ_{CLS} is the classification’s parameters, M indicates the matching label: specifically, $M = 1$ if the label of \mathbf{X}_1 equals that of \mathbf{X}_2 , otherwise $M = 0$. Here, n is the mini-batch size, and $D_{\theta_{CLS}}$ is the Euclidean distance of the two representation vectors. m represents the threshold ($m=2$), while P signifies feature dimension.

In SSL-V3, Contrastive loss measures the discrepancy between the two branches. Contrastive loss leverages the contrastive structure and examines the relationship between samples within the current batch as well. In addition, the Contrastive loss is

characterized by less complex factors and a simpler format. The BCE loss serves as a subject-level loss, computes the prediction loss subject by subject, and accumulates them together.

4 Experiments

In this section, we first introduce the datasets, evaluation metrics, and implementation details. Then, we conduct the experiments and ablation study, and evaluate the results.

4.1 Dataset and Processing

I-CONNECT dataset The Internet-Based Conversational Engagement Clinical Trial (I-CONNECT) contains a video dataset for the detection of Mild Cognitive Impairment (MCI) detection task² [2, 37]. Each sample is a 30-minute theme-oriented interview video between the interviewee (subject) and the interviewer. I-CONNECT convened 186 subjects older than 75, including 100 with MCI and 86 with Normal Cognition (NC) (ClinicalTrials.gov #: NCT02871921).

However, the video quality varies significantly from subject to subject as they were recorded with different cameras, recording speeds and resolutions, and indoor lighting conditions. High-resolution videos result in more robust predictions than blurred ones [2], which motivates us to study whether referring to video quality benefits prediction. Hence, I-CONNECT is appropriate for testing the proposed SSL-V3 framework.

This paper focuses on 4 themes: Crafts Hobbies, Day Time TV Shows, Movie Genres, and School Subjects. Table 1 presents the data distribution.

Table 1: The details of researched themes. Subject Number is the total number of videos in the corresponding theme. Male/Female and MCI/NC show the gender distribution and category distribution. Frame Number is the total image number of each theme after converting videos into frames.

	Crafts Hobbies	Day Time TV Shows	Movie Genres	School Subjects
Subject Number	32	41	35	39
Male/Female	11/21	11/30	10/25	11/28
MCI/NC	20/12	20/21	21/14	22/17
Frame Number	691872	859872	770656	797968

Typically, in each video, the subject exhibits normal cognition at the start and the end, introducing many noisy features that reduce accuracy. To avoid interfering, we discard the first 3 minutes and the last 2.5 minutes of each video. Then, Fig. 4 states that every video has a complex background and interviewer’s face. To focus on the subject’s facial expression, we employed EasyOCR+RetineFace [38] to crop the interviewees’ facial images and exclude all other information.

²Website: <https://www.i-connect.org/>.

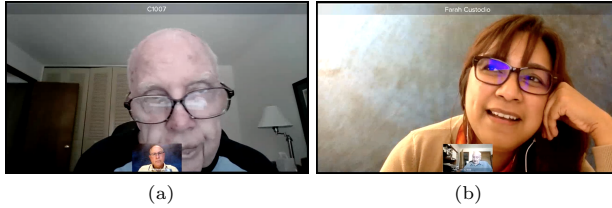


Fig. 4: Two sample frames from the I-CONNECT dataset. In (a), the window of the interviewee is bigger than that of the interviewer because the interviewer was speaking. Conversely, in (b), the interviewer was talking so that her window was bigger than the interviewee’s.

Simultaneously, inspired by [39, 40], this study uses sequence-based approaches, taking consecutive frames as the input and setting the frame number as 16. To fully leverage the videos, we use K-fold Cross Validation. Table 2 specifies the fold number for each theme. Additionally, the videos in each fold belong to different subjects.



Fig. 5: More subjects from Hockey Fight Detection dataset. The upper line represents high-quality frames. The bottom line stands for poor-quality frames.

Hockey Fight Detection dataset

Fighting involves high-speed body motion, resulting in blurred and low-quality video, which can lead to mediocre predictions. To validate the generalization of SSL-V3, we also use the Hockey Fight Detection (HF) dataset [41] as a secondary dataset to determine if SSL-V3 can achieve reasonable results.

The HF dataset assesses fight and violence in the hockey games of the National Hockey League. It contains 1000 video clips with a resolution of 360×288 pixels. Each video lasts between 1 and 2 seconds with a frame rate of 25 FPS. The HF dataset contains two categories: 500 fights and 500 non-fights. Fig. 6 shows examples of both fight and non-fight clips.

Similar to the I-CONNECT dataset, we also use sets of adjacent 16 frames as input. We then randomly divide the dataset into training, validation, and test sets in an 8:1:1 ratio, and report the mean and standard deviation (STD) values from five randomized experiments.



Fig. 6: Two samples from ^(a)HF dataset. (a) is the scenario of fighting action. (b) presents the normal non-fight situation.

4.2 Evaluation Metrics

This work employs five typical metrics - Prediction accuracy, F1 score, AUC (Area Under the Receiver Operating Characteristic Curve), Sensitivity, and Specificity - to evaluate classification performance.

4.3 Implementation Details

We split the input clips into several low-resolution cubic patches. Then, we augment the input cubes in various ways (random horizontal and vertical flip, random rotation, center crop, and color space augmentations) for two branches. Next, SSL-V3 shuffles and permutes the clips within the input mini-batch to generate the second input. Two branches accept the two inputs individually. Here, CBS Loss supervises the training process. The batch size is 80 for the I-CONNECT dataset and 40 for the HF dataset, with an input frame length of 16. The initialized learning rate is $1e-8$. We used the Adam optimizer and Cyclic scheduler with the triangular2 mode. The epoch number is 50. We implemented the model using PyTorch 1.12.0+cu116 and conducted experiments on an NVIDIA GTX 3090 GPU.

4.4 MCI Detection

MCI is an international public health issue. Worldwide, up to 15.56% of community dwellers aged over 50 years are affected by MCI [42]. Furthermore, 21.2% older adults in nursing homes have MCI [43]. Efficient early detection of MCI is urgently needed. Hence, we apply SSL-V3 to this healthcare topic to test if SSL-V3 can efficiently detect MCI from NC in each theme.

Table 2 shows the specific results. All accuracies from SSL-V3 are over 88%. For example, on the theme of School Subjects, SSL-V3 successfully predicts 37 out of 39 cases, achieving the highest accuracy of 94.87%. It also reaches 93.75% accuracy on the Crafts Hobbies, which is close to 94%. Additionally, the strong results of the rest metrics also solidly support that SSL-V3 has robust performance and can reliably and balancedly predict positive and negative samples with the help of video quality score. Table 3 also indicates that SSL-V3 outperforms the other models and referring to VQA significantly benefits the prediction.

Table 2: The prediction accuracy of detecting MCI on 4 themes using K-fold evaluation.

Test Theme	Crafts Hobbies	Day Time TV Shows	Movie Genres	School Subjects
Fold Num	11	14	11	13
Accuracy	30/32	37/41	31/35	37/39
F1	93.75%	90.24%	88.57%	94.87%
AUC	95.00%	90.00%	91.30%	95.65%
MCI/NC	93.33%	90.24%	88.90%	94.12%
Sensitivity/	20/12	20/21	21/14	22/17
Specificity	95%/	90%/	95.45%/	100%/
	91.67%	90.48%	82.35%	88.24%

Table 3: Compare the performance of SSL-V3 with other models on the I-CONNECT dataset. No VQA means to classify the videos without referring to the video quality, while VQA represents using VQA to classify videos.

	Data Modality	Accuracy	F1
Chen <i>et al.</i> [44]	Text	79.15%	-
Liu <i>et al.</i> [45]	Text, MRI	87.00%	89.00%
Alsuhaibani <i>et al.</i> [3]	Video	87.50%	89.00%
MC-ViViT [2]	Video	90.63%	93.03%
SSL-V3 (No VQA)	Video	87.80%	86.49%
SSL-V3 (VQA)	Video	94.87%	95.65%

4.5 Violence Detection

Violence detection, as a part of human action recognition at a distance, is an important topic in surveillance. It is crucial for public safety. Therefore, we validate SSL-V3 on the HF dataset to detect violent actions.

Table 4: The prediction accuracy of detecting violence on HF dataset. The report format is mean \pm STD%

Accuracy	F1	AUC	Sensitivity	Specificity
98.6 \pm 0.8%	98.59 \pm 0.81%	98.6 \pm 0.8%	98.0 \pm 1.26%	99.2 \pm 0.99%

Table 4 presents that SSL-V3 achieved promising results on all five metrics, all mean values are over 98% with low standard deviations (STD), indicating the robustness of SSL-V3 in detecting positive and negative samples. Moreover, according to Table 5, our mean accuracy of 98.6% with an STD of 0.008 is comparable to the top-1 accuracy achieved by SepConvLSTM-C [46] (99.5%). The joining of VQA devoted to the good result a lot. Therefore, SSL-V3 can efficiently detect fighting during hockey games.

4.6 Ablation Study

The ablation study is conducted on the I-CONNECT and HF datasets.

Table 5: Compare the performance of other models with SSL-V3 on the HF dataset.

	Accuracy	F1
CNN+SVM [47]	93.7%	-
2D CNN [48]	94.60±0.6%	-
MobileNet [49]	96.66%	-
C3D+SVM [50]	97.86%	97.87%
Computationally Intelligent VD [51]	98%	98.10%
Spatial Encoder [52]	98.1±0.58%	-
3D CNN [53]	98.3±0.81%	-
SepConvLSTM-C [46]	99.5%	-
SSL-V3 (No VQA)	95.0±1.41%	94.98±1.36%
SSL-V3 (VQA)	98.6±0.8%	98.59±0.81%

4.6.1 Study the essential of VQA task

This study investigates the impact of the VQA task. Testing the model without the intervention of VQA involves using neither SSR nor VSR, the first row of Table 6.

Table 6: The prediction accuracy on 4 I-CONNECT themes and HF dataset with different regressors. SSR and VSR denotes Sequence Score Regressor and Video Score Regressor respectively.

SSR	VSR	Crafts Hobbies	Day Time TV Shows	Movie Genres	School Subjects	Hockey Fight
✓	✓	84.38%	87.80%	80.00%	82.05%	(95±1.41)%
✓		87.50%	78.05%	88.57%	84.62%	(95.6±1.36)%
	✓	87.50%	87.80%	82.86%	76.92%	(95.6±2.5)%
✓	✓	93.75%	90.24%	88.57%	94.87%	(98.6±0.8)%

Table 6 demonstrates that, across all themes, VQA head contributes to significant improvement in the performance of SSL-V3. For instance, the VQA head provides more than 8.5% improvement in accuracy for SSL-V3 in the Crafts Hobbies and Movie Genres. The increase is even 12.82% in the School Subjects. Therefore, referring to VQA significantly benefits the model’s prediction accuracy, underscoring the necessity of considering video quality in video classification. The results from the HF dataset also support this conclusion (Table A3).

At the same time, Table 6 supports that VQA auxiliary improves the learned representation and downstream performance instead of causing harmful over-fitting to augmentation artifacts. Importantly, in all experiments, no data augmentation is applied at inference time, yet the model consistently achieves strong performance. Since the VQA head operates on clean inputs at inference, if it had relied on augmentation-specific artifacts learned during training, its outputs and the resulting classification would be expected to degrade under this distribution shift; however, this behavior is not observed. Hence, augmentation artifacts are incorporated as controlled, task-aligned degradation signals (not contradictory supervision), and both the method design and ablation Table 6, together with the strong clean-inference performance, support that they regularize - rather than shortcut - the learned representation

4.6.2 Study the best structure of VQA head

This study investigates the necessity of VQA head’s two modules, SSR and VSR. Tang *et al.* [36] and Kim *et al.* [15] tuned the parameters of each module respectively.

In the case of using VSR alone, SSR is replaced with a 1D average pooling layer, which operates on the extracted features of each sequence. Conversely, when using SSR alone, the VSR module is replaced with a single FC layer that directly regresses the output of SSR to the overall clip quality score.

Table 6 indicates that using the VQA head results in better performance than using either SSR or VSR alone. For example, the accuracy of the VQA head is consistently at least 2.44% higher than that of VSR alone. While the VQA head and SSR alone achieve comparable accuracy in Movie Genres, the VQA head consistently outperforms SSR alone by at least 6.25% across other themes.

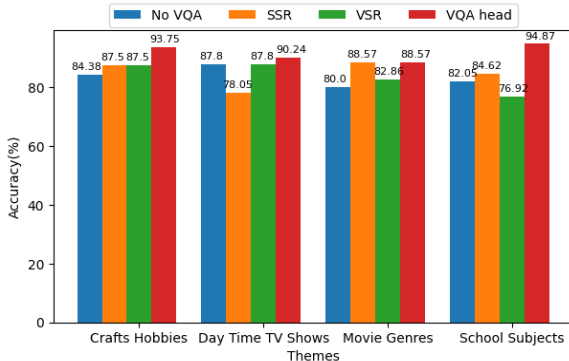


Fig. 7: The prediction accuracy on 4 themes (I-CONNECT dataset) with different regressors.

Between the two modules, SSR alone performs better than VSR alone in Movie Genres and School Subjects and ties with VSR alone in Crafts Hobbies. Specifically, in School Subjects, adding the VSR module brings a 10.25% accuracy increase to the SSL-V3, while adding SSR provides approximately an 18% improvement in accuracy. This highlights the effectiveness of SSR in enhancing performance over VSR. Fig. 7 reflects this disparity. SSR learns raw Spatio-Temporal features, whereas replacing SSR with 1D average pooling removes specific characteristics from the features, hindering VSR’s ability to make precise decisions. Hence, SSR alone outperforms VSR alone. We draw the same conclusion from HF dataset. The specific results in Tables A2 and A3 from Appendix A support this view as well.

Overall, the VQA head enhances SSL-V3’s performance substantially compared to using either SSR or VSR alone. Within the VQA head, SSR is more effective than VSR.

4.6.3 Study the effectiveness of contrastive structure

This study inspects the essence of using the contrastive structure in Combined-SSL. Discarding the contrastive structure involves removing the Contrastive loss from the CBS Loss.

Table 7: The prediction accuracy on 4 I-CONNECT themes and HF dataset with different loss functions. CL means Contrastive Learning.

FL	CL Loss	BCE Loss	Crafts Hobbies	Day Time TV Shows	Movie Genres	School Subjects	Hockey Fight
✓			81.25%	65.85%	54.29%	51.28%	(92.8±1.6)%
✓	✓		84.38%	85.37%	71.43%	79.49%	(94.4±1.96)%
✓		✓	81.25%	68.29%	71.43%	69.23%	(94.2±1.47)%
✓	✓	✓	93.75%	90.24%	88.57%	94.87%	(98.6±0.8)%

Table 7 shows that the contrastive structure substantially enhances the performance of SSL-V3. Across all themes, using the contrastive structure enables SSL-V3 to be at least 12.5% more accurate than when it is discarded. This accords to the pattern of the results from HF dataset. Contrastive Learning is indispensable for Combined-SSL.

4.6.4 Study suitable loss function

This study evaluates the effect of various loss functions to determine the best one for SSL-V3. FL is the base of CBS Loss, with Contrastive loss and BCE losses serving as supplementary components. Except for purely FL, we combine FL with Contrastive loss and BCE alternately to test the effects of the two combinations.

Table 7 shows that CBS Loss outperforms the other combination on both datasets. For instance, in Movie Genres, CBS Loss achieves its lowest accuracy at 88.57%, which is 34.28% larger than the accuracy of FL alone and approximately 17.1% higher than those of FL + BCE and FL + Contrastive loss, both at 71.43%. This disparity indicates the significance of using Contrastive loss and Subject-level loss.

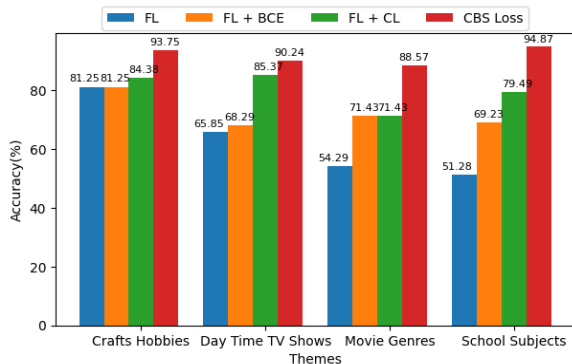


Fig. 8: The prediction accuracy on 4 themes (I-CONNECT dataset) with different loss functions. CL means Contrastive Learning.

Both FL + BCE and FL + Contrastive loss outperform FL alone across the overall themes (Fig. 8). With Contrastive loss included, FL + Contrastive loss achieved 3.13% and 10.26% higher accuracy on Crafts Hobbies and School Subjects, respectively, compared to using FL + BCE. Thus, Contrastive loss is important, also supported by the results of HF dataset, highlighting that the batch-level loss forms the foundation part. When BCE loss, which operates at the subject level, is incorporated, SSL-V3 demonstrates improved performance. Without Contrastive loss, empowering the model and enhancing predictions at the subject level becomes challenging, largely due to unresolved intra-class imbalance issues. Contrastive loss effectively addresses intra-class imbalances within the mini-batch context. Furthermore, discarding the Contrastive loss is equivalent to removing the contrastive structure, which substantially decreases the performance of SSL-V3, demonstrating the importance of Contrastive loss. All results in Tables A1 and A3 from Appendix A strongly support this conclusion.

In summary, the results of the ablation study support selecting CBS Loss.

4.6.5 Compare the impact of CBS Loss to that of VQA head

Table 7 implies that with the VQA head and partial CBS Loss, SSL-V3 struggles to achieve over 80% accuracy in all themes except Crafts Hobbies.

Table 6 illustrates that with CBS Loss and a partial VQA head, SSL-V3 achieves over 80% accuracy effortlessly. Despite this, VSR alone achieves 76.92% on School Subjects, which ranks as the fourth highest value among FL alone, FL+BCE, and FL+Contrastive Learning in Table 7.

Hence, comparing the two tables indicates that CBS Loss has a greater impact on SSL-V3 than the VQA head does. In essence, a robust loss function is more crucial than a high-performing classifier or regressor head.

5 Discussion

SSL-V3 is designed for two tasks: VQA and classification, making it a potential multi-task model. Both tasks train the same ViViT together, driving it to learn video content from diverse perspectives. Moreover, the collaboration of each module also leads to SSL-V3’s robust performance in MCI detection and violence detection.

Specifically, **Combined-SSL** optimizes VQA and classification reciprocally, effectively addressing the label shortage in the VQA task. In addition, the contrastive structure helps to tune the VQA task comprehensively and emphasizes making features from the same group denser and those from opposite classes more separable. **VQA head** highlights the effect of important features by the SSR module and fuses the temporal effect across different channels stereoscopically.

ViViT, with the shared weight mechanism, extracts a diverse and rich set of Spatio-Temporal features to meet the demands of VQA and classification. Fig. 9 shows that ViViT pays particular attention to muscle motion in the cheek and brow bone regions within the I-CONNECT dataset (Fig. 9a). ViViT also focuses on muscle motions in other areas like the forehead, nose, eyelids, and lips. Additionally, in the HF dataset, Fig. 9b suggests that ViViT highlights body motion in the fighting video. In contrast,

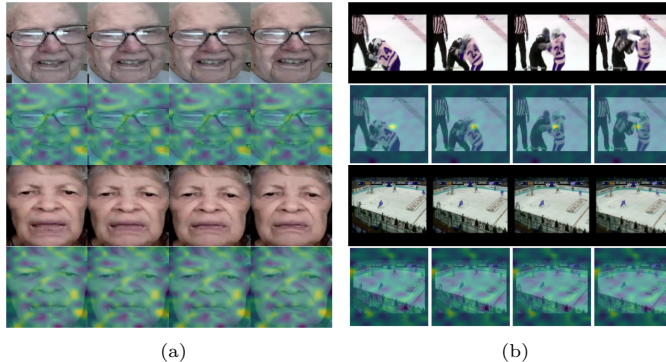


Fig. 9: The extracted spatio-temporal feature maps on 16 consecutive frames from two datasets. SSL-V3 focuses more on the bright areas and less on the dark ones. Given that there are n_t tubelets, where $n_t = \frac{T}{t} = \frac{16}{4} = 4$, there are four feature maps. To simplify the visualization, we pick the first frame of each tubelet to represent it. Fig. 9a is from the I-CONNECT dataset, while Fig. 9b is from HF one.

in non-fighting videos, SSL-V3 tends to capture the movement of single objects and the environment of the court.

The **CBS Loss** optimizes SSL-V3 at both Batch and Subject levels. Notably, using the contrastive structure, CBS loss solves the intra-class imbalance issue at the mini-batch level. Additionally, it requires no memory bank, making it space- and computation-efficient.

In summary, there are five key findings or strengths.

- Referring to video quality scores benefits the neural network in classification over existing models.
- Noval Combined-SSL alleviates the pressure of label scarcity in VQA.
- Contrastive Learning improves model performance and addresses class imbalance issues.
- SSL-V3 has strong generalization across domains (healthcare and surveillance).
- SSL-V3 is scalable. ViViT’s property on sequential video processing enables the SSL-V3 to classify longer video and execute real-time constraint on each clip.

6 Conclusion and Future Work

This paper developed SSL-V3 based on the proposed Combined-SSL to perform video classification by referring to the video quality score. Combined-SSL uses video quality score as a factor to tune the classification task and applies a contrastive structure to improve performance. SSL-V3 also impresses people by practical applicability. The good experimental results from the I-CONNECT and HF datasets verify the effectiveness of SSL-V3 on real-world noisy video streams in healthcare and surveillance. Considering video quality is the right move while doing classification.

Simultaneously, we would like to highlight that different from Pretext Task and Contrastive Learning, Combined-SSL drops the fine-tuning part. Moreover, the designing logic behind Combined-SSL offers a new way to address the label shortage issue, which is combining the target task with one or even more tasks with sufficient labels.

However, this study has limitations.

- **SSL-V3 is not a fully multi-task model**

Due to missing labels, it is difficult to evaluate the computed video quality score using metrics like Spearman’s Rand-order Correlation Coefficient, Pearson Linear Correlation Coefficient, and Root Mean Squared Error. Hence, it is hard to claim that SSL-V3 is a fully multi-task model.

- **Referring to the video quality score is not panacea**

The prediction of all perfect-quality video is surely better than that of referring to the video quality score.

- **Potential overfitting**

The SSL-V3 may suffer from overfitting issue while processing datasets with small subject number and short video clips.

Hence, future work will focus on experimenting with SSL-V3 on public video datasets with both category labels and video quality scores to verify that SSL-V3 is a generalized SSL multi-task model. Then, the importance of video quality suggests that even a simple neural network can achieve good accuracy with high-quality video. Another research direction is to perform video denoising using a generative model before classification. This way helps skip the video quality part and generate high-quality video, promising good and objective performance for sure.

Acknowledgments. The collection of the I-CONNECT dataset was partly supported by the National Institute of Health (NIH) funding: R01AG051628 and R01AG056102.

Declarations

Funding Not applicable

Conflict of interest The authors have no relevant financial or non-financial interests to disclose.

Ethics approval Not applicable

Consent for publication Not applicable

Data availability I-CONNECT dataset will be made available on request through <https://www.i-connect.org/>.

Hockey Fight Detection Dataset is a public dataset

(<https://paperswithcode.com/dataset/hockey-fight-detection-dataset>).

Materials availability Not applicable

Appendix A Full Results of Ablation Study

Table A1 states the full results of tuning loss functions. FL + Contrastive loss achieves better Accuracy, F1, and Specificity than FL + BCE in the Crafts Hobbies and School Subjects themes. In the remaining two themes, FL + Contrastive loss and FL +

Table A1: Specific results on 4 themes with different loss functions. CL means Contrastive Learning.

Test Themes	Crafts Hobbies			Day Time TV Shows		
	FL	FL + BCE	FL + CL	FL	FL + BCE	FL + CL
Accuracy	26/32	26/32	27/32	27/41	28/41	28/41
F1	81.25%	81.25%	84.38%	65.85%	68.29%	85.37%
AUC	82.35%	84.21%	85.71%	50.00%	68.29%	85.00%
MCI/NC	85.00%	81.67%	87.50%	65.12%	68.33%	85.36%
Sensitivity/		20/12			20/21	
Specificity	70.00%/	80.00%/	75.00%/	35.00%/	70.00%/	85.00%/
	100.00%	83.33%	100.00%	95.24%	66.67%	85.71%
Test Themes	Movie Genres			School Subjects		
	FL	FL + BCE	FL + CL	FL	FL + BCE	FL + CL
Accuracy	19/35	25/35	25/35	20/39	27/39	31/39
F1	54.29%	71.43%	71.43%	51.28%	69.23%	79.49%
AUC	46.66%	77.27%	77.27%	38.71%	75.00%	81.82%
MCI/NC	59.52%	69.05%	69.05%	53.57%	68.25%	79.37%
Sensitivity/		21/14			22/17	
Specificity	33.33%/	80.95%/	80.95%/	27.27%/	81.82%/	81.82%/
	85.71%	57.14%	57.14%	82.35%	52.94%	76.47%

BCE are tied. Overall, FL + Contrastive loss surpasses FL + BCE, indicating that addressing class imbalance issues takes priority over considering subject-level loss. Contrastive loss is more critical.

Table A2: Specific results on 4 themes with different regression head.

Test Themes	Crafts Hobbies			Day Time TV Shows		
	No VQA	VSR	SSR	No VQA	VSR	SSR
Accuracy	27/32	28/32	28/32	36/41	36/41	32/41
F1	84.38%	87.50%	87.50%	87.80%	87.80%	78.05%
AUC	87.18%	90.00%	90.00%	86.49%	87.18%	78.05%
MCI/NC	86.67%	86.67%	86.67%	87.62%	87.74%	78.10%
Sensitivity		20/12			20/21	
Specificity	85.00%	90.00%	90.00%	80.00%	85.00%	80.00%
	83.33%	83.33%	83.33%	95.24%	90.48%	76.19%
Test Themes	Movie Genres			School Subjects		
	No VQA	VSR	SSR	No VQA	VSR	SSR
Accuracy	28/35	29/35	31/35	32/39	30/39	33/39
F1	80.00%	82.86%	88.57%	82.05%	76.92%	84.62%
AUC	82.05%	86.96%	90.48%	82.92%	75.68%	85.72%
MCI/NC	80.95%	79.76%	88.10%	84.92%	78.17%	84.92%
Sensitivity		21/14			22/17	
Specificity	76.19%	95.24%	90.48%	77.27%	63.64%	81.82%
	85.71%	64.29%	85.71%	88.24%	94.12%	88.24%

Table A2 contains all the metrics for tuning the regressor head. SSR and VSR reached better metric values than No VQA across the board. Focusing on SSR and

VSR, in Crafts Hobbies and Day Time TV Shows, VSR alone performs better than or identical to SSR alone across all the metrics. However, in Movie Genres and School Subjects, SSR alone surpasses VSR alone in Accuracy and F1 score. They are tied in AUC. Furthermore, SSR alone achieves better Specificity in Movie Genres and higher Sensitivity in School Subjects than VSR alone. In summary, SSR alone leads to better performance than VSR alone, implying that SSR contributes more to SSL-V3.

Table A3: Specific results on HF dataset with different loss functions and regressors. CL means Contrastive Learning.

Test Themes	Study Loss Function		
	FL	FL + CL	FL + BCE
Accuracy	(92.80±1.60)%	(94.40±1.96)%	(94.20±1.47)%
F1	(92.92±1.74)%	(94.38±1.96)%	(94.19±1.47)%
AUC	(92.80±1.60)%	(94.40±1.96)%	(94.20±1.47)%
Sensitivity/	(90.80±3.71)%/	(94.00±4)%/	(94.00±2.53)%/
Specificity	(94.80±2.04)%	(94.80±4.31)%	(94.40±2.93)%
Test Themes	Study VQA head		
	No VQA	SSR	VSR
Accuracy	(95.00±1.41)%	(96.40±1.36)%	(95.60±2.50)%
F1	(94.98±1.36)%	(96.41±1.36)%	(95.56±2.53)%
AUC	(94.60±1.36)%	(96.40±1.36)%	(95.60±2.50)%
Sensitivity/	(94.40±2.33)%/	(96.80±1.60)%/	(94.80±2.99)%/
Specificity	(95.60±3.20)%	(96.00±1.26)%	(96.40±2.65)%

Table A3 contains all the results of ablation study from HF dataset. We can draw the same conclusion as Tables A1 and A2 do.

Appendix B What does last batch mean? How does per-subject aggregation?

Supposing there are 1000 batches in one epoch from batch 1 to batch 1000. The 1000th batch is the last batch in our case.

For a given batch, it contains clips from different subjects. To compute the subject-level loss, it requires to collect the prediction results of all clips. In the last batch of the current epoch (like 1000th batch), we finish collecting the results of all clips for each subject. Then we can start computing subject-level loss.

Supposing batch size = 4, $\hat{Y}_{b_i} = [s_{10}, s_5, s_{15}, s_{20}]$, $GT_{b_i} = [gt_1, gt_2, gt_3, gt_4]$, where \hat{Y}_{b_i} is the predicted results of i^{th} batch b_i , s_j is each predicted subject index, GT_{b_i} is the ground truth vector of i^{th} batch b_i , gt_j is each ground truth category ($i, j \in \mathbf{N}^+$).

If $s_{10} = gt_1$, we say the model predicts this clip to a correct category and mark it as 1. Otherwise, it is 0. We create a list acc_num to accumulately count the correct predicted number for each subject batch by batch. In the meanwhile, we use list cnt to count all clip number of each subject.

In the last batch, we use this formula, $acc_total = \text{round}(acc_num/cnt)$, to calculate the subject-level accuracy acc_total for each subject. If the accuracy of certain subject is larger than 0.5, we round it to 1 (correct). Otherwise, it is 0 (wrong).

Then, we use acc_total and overall ground truth result to compute binary cross entropy loss as the subject-level loss.

Appendix C Glossary

Table C4 explains the detail of acronyms in this paper.

Table C4: Glossary

Initials	Vocabulary
AD	Alzheimer’s Disease
ADRD	Alzheimer’s Disease Related Dementia
BEEF	Bidirectional Effect-Based Fusion
CBS Loss	Combined Batch- and Subject-level Loss
CLS	Classification
HF	Hockey Fight Detection
MC	Multi-branch Classifier
MCI	Mild Cognitive Impairment
MOS	Mean Option Scores
NC	Normal Cognition
NR-VQA	No-Reference Video Quality Assessment
SQS	Sequence Quality Score
SSL	Self-Supervised Learning
SSL-V3	Self-Supervised Learning-based NR-VQA Combined with ViViT for Video Classification
SSR	Sequence Score Regressor
VQA	Video Quality Assessment
VQS	Video Quality Score
VSR	Video Score Regressor

References

- [1] Gao, T., Zhang, M., Zhu, Y., Zhang, Y., Pang, X., Ying, J., Liu, W.: Sports video classification method based on improved deep learning. Applied Sciences **14**(2) (2024) <https://doi.org/10.3390/app14020948>
- [2] Sun, J., Dodge, H.H., Mahoor, M.H.: Mc-vivit: Multi-branch classifier-vivit to detect mild cognitive impairment in older adults using facial videos. Expert Systems with Applications, 121929 (2023)
- [3] Alsuhaibani, M., Dodge, H.H., Mahoor, M.H.: Mild cognitive impairment detection from facial video interviews by applying spatial-to-temporal attention module. Expert Systems with Applications **252**, 124185 (2024)

- [4] Jiang, S., Sang, Q., Hu, Z., Liu, L.: Self-supervised representation learning for video quality assessment. *IEEE Transactions on Broadcasting* **69**(1), 118–129 (2023) <https://doi.org/10.1109/TBC.2022.3197904>
- [5] Mitra, S., Soundararajan, R.: Multiview contrastive learning for completely blind video quality assessment of user generated content. In: *Proceedings of the 30th ACM International Conference on Multimedia. MM '22*, pp. 1914–1924. Association for Computing Machinery, New York, NY, USA (2022). <https://doi.org/10.1145/3503161.3548064> . <https://doi.org/10.1145/3503161.3548064>
- [6] Chen, Y.-C., Saha, A., Davis, C., Qiu, B., Wang, X., Gowda, R., Katsavounidis, I., Bovik, A.C.: Gamival: Video quality prediction on mobile cloud gaming content. *IEEE Signal Processing Letters* **30**, 324–328 (2023)
- [7] Mi, Y., Li, Y., Shu, Y., Liu, S.: Ze-fesg: A zero-shot feature extraction method based on semantic guidance for no-reference video quality assessment. In: *ICASSP 2024-2024 IEEE International Conference on Acoustics, Speech and Signal Processing (ICASSP)*, pp. 3640–3644 (2024). IEEE
- [8] Campos, W., Saavedra, J.M., Stears, C.: A study on self-supervised sketch-based image retrieval on unpaired data (s3bir). *Neural Computing and Applications*, 1–19 (2025)
- [9] Jayamohan, M., Yuvaraj, S.: A novel human actions recognition and classification using semantic segmentation with deep learning techniques. *Neural Computing and Applications*, 1–17 (2025)
- [10] Arnab, A., Deghani, M., Heigold, G., Sun, C., Lučić, M., Schmid, C.: Vivit: A video vision transformer. In: *Proceedings of the IEEE/CVF International Conference on Computer Vision*, pp. 6836–6846 (2021)
- [11] Xu, M., Li, C., Zhang, S., Callet, P.L.: State-of-the-art in 360° video/image processing: Perception, assessment and compression. *IEEE Journal of Selected Topics in Signal Processing* **14**(1), 5–26 (2020) <https://doi.org/10.1109/JSTSP.2020.2966864>
- [12] Zhang, B., Chen, J., Xu, Y., Zhang, H., Yang, X., Geng, X.: Auto-encoding score distribution regression for action quality assessment. *Neural Computing and Applications* **36**(2), 929–942 (2024)
- [13] Schlett, T., Rathgeb, C., Henniger, O., Galbally, J., Fierrez, J., Busch, C.: Face image quality assessment: A literature survey. *ACM Computing Surveys (CSUR)* **54**(10s), 1–49 (2022)
- [14] Imani, H., Islam, M.B., Arica, N.: Three-stream 3d deep cnn for no-reference stereoscopic video quality assessment. *Intelligent Systems with Applications* **13**, 200059 (2022) <https://doi.org/10.1016/j.iswa.2021.200059>

- [15] Kim, H.G., Lim, H.-T., Ro, Y.M.: Deep virtual reality image quality assessment with human perception guider for omnidirectional image. *IEEE Transactions on Circuits and Systems for Video Technology* **30**(4), 917–928 (2020) <https://doi.org/10.1109/TCSVT.2019.2898732>
- [16] Sun, W., Wang, T., Min, X., Yi, F., Zhai, G.: Deep learning based full-reference and no-reference quality assessment models for compressed ugc videos. In: 2021 IEEE International Conference on Multimedia & Expo Workshops (ICMEW), pp. 1–6. IEEE Computer Society, Los Alamitos, CA, USA (2021). <https://doi.org/10.1109/ICMEW53276.2021.9455999> . <https://doi.ieeecomputersociety.org/10.1109/ICMEW53276.2021.9455999>
- [17] Tan, Y., Kong, G., Duan, X., Long, H., Wu, Y.: No-reference video quality assessment based on spatio-temporal perception feature fusion. *Neural Processing Letters* (2022) <https://doi.org/10.1007/s11063-022-10939-x>
- [18] Zhang, L., Zhou, K., Lu, F., Li, Z., Shao, X., Zhou, X.-D., Shi, Y.: Esmformer: Error-aware self-supervised transformer for multi-view 3d human pose estimation. *Pattern Recognition* **158**, 110955 (2025)
- [19] Mao, W., Liu, K., Zhang, Y., Liang, X., Wang, Z.: Self-supervised deep tensor domain-adversarial regression adaptation for online remaining useful life prediction across machines. *IEEE Transactions on Instrumentation and Measurement* **72**, 1–16 (2023) <https://doi.org/10.1109/TIM.2023.3265109>
- [20] Yang, Q., Wang, C., Liu, P., Jiang, Z., Li, J.: Video anomaly detection via self-supervised and spatio-temporal proxy tasks learning. *Pattern Recognition* **158**, 111021 (2025)
- [21] Kwong, N.-W., Chan, Y.-L., Tsang, S.-H., Lun, D.P.-K.: Optimized quality feature learning for video quality assessment. In: ICASSP 2023 - 2023 IEEE International Conference on Acoustics, Speech and Signal Processing (ICASSP), pp. 1–5 (2023). <https://doi.org/10.1109/ICASSP49357.2023.10095975>
- [22] Tarvainen, A., Valpola, H.: Mean teachers are better role models: Weight-averaged consistency targets improve semi-supervised deep learning results. *Advances in neural information processing systems* **30** (2017)
- [23] Pozzi, A., Incremona, A., Tessera, D., Toti, D.: Mitigating exposure bias in large language model distillation: an imitation learning approach. *Neural Computing and Applications*, 1–17 (2025)
- [24] Chen, T., Kornblith, S., Norouzi, M., Hinton, G.: A simple framework for contrastive learning of visual representations. In: International Conference on Machine Learning, pp. 1597–1607 (2020). PMLR

- [25] He, K., Fan, H., Wu, Y., Xie, S., Girshick, R.: Momentum contrast for unsupervised visual representation learning. In: Proceedings of the IEEE/CVF Conference on Computer Vision and Pattern Recognition, pp. 9729–9738 (2020)
- [26] Chen, X., Fan, H., Girshick, R., He, K.: Improved baselines with momentum contrastive learning. arXiv preprint arXiv:2003.04297 (2020)
- [27] Chen, X., Xie, S., He, K.: An empirical study of training self-supervised vision transformers. 2021 IEEE/CVF International Conference on Computer Vision (ICCV), 9620–9629 (2021)
- [28] Meng, T., Ai, W., Li, J., Wang, Z., Li, K.: Se-gcl: an event-based simple and effective graph contrastive learning for text representation. Neural Computing and Applications, 1–14 (2025)
- [29] Wang, J., Yoshie, O., Ieiri, Y.: Conducting patch contrastive learning with mixture of experts on mixed datasets for medical image segmentation. Neural Computing and Applications, 1–28 (2025)
- [30] Zhao, J., Mathieu, M., LeCun, Y.: Energy-based generative adversarial networks. In: International Conference on Learning Representations (2017). <https://openreview.net/forum?id=ryh9pmcee>
- [31] Feichtenhofer, C., Fan, H., Xiong, B., Girshick, R., He, K.: A large-scale study on unsupervised spatiotemporal representation learning. In: Proceedings of the IEEE/CVF Conference on Computer Vision and Pattern Recognition, pp. 3299–3309 (2021)
- [32] Feng, Y., Li, S., Chang, Y.: Multi-scale feature-guided stereoscopic video quality assessment based on 3d convolutional neural network. In: ICASSP 2021 - 2021 IEEE International Conference on Acoustics, Speech and Signal Processing (ICASSP), pp. 2095–2099 (2021). <https://doi.org/10.1109/ICASSP39728.2021.9414231>
- [33] Sun, J., Fard, A.P., Mahoor, M.H.: Xnodr and xnidr: Two accurate and fast fully connected layers for convolutional neural networks. Journal of Intelligent & Robotic Systems **109**(1), 17 (2023)
- [34] Lin, E., Sun, J., Chen, H., Mahoor, M.H.: Data quality matters: Suicide intention detection on social media posts using roberta-cnn. In: 2024 46th Annual International Conference of the IEEE Engineering in Medicine and Biology Society (EMBC), pp. 1–5 (2024). IEEE
- [35] Alsuhaibani, M., Fard, A.P., Sun, J., Poor, F.F., Pressman, P.S., Mahoor, M.H.: A review of machine learning approaches for non-invasive cognitive impairment detection. IEEE Access (2025)

- [36] Tang, J., Dong, Y., Xie, R., Gu, X., Song, L., Li, L., Zhou, B.: Deep blind video quality assessment for user generated videos. In: 2020 IEEE International Conference on Visual Communications and Image Processing (VCIP), pp. 156–159 (2020). <https://doi.org/10.1109/VCIP49819.2020.9301757>
- [37] Wu, C.-Y., Mattek, N., Wild, K., Miller, L.M., Kaye, J.A., Silbert, L.C., Dodge, H.H.: Can changes in social contact (frequency and mode) mitigate low mood before and during the covid-19 pandemic? the i-conect project. *Journal of the American Geriatrics Society* **70**(3), 669–676 (2022)
- [38] Deng, J., Guo, J., Ververas, E., Kotsia, I., Zafeiriou, S.: Retinaface: Single-shot multi-level face localisation in the wild. In: Proceedings of the IEEE/CVF Conference on Computer Vision and Pattern Recognition, pp. 5203–5212 (2020)
- [39] Liu, D., Zhang, H., Zhou, P.: Video-based facial expression recognition using graph convolutional networks. 2020 25th International Conference on Pattern Recognition (ICPR), 607–614 (2021)
- [40] Mohan, B., Popa, M.: Temporal based emotion recognition inspired by activity recognition models. In: 2021 9th International Conference on Affective Computing and Intelligent Interaction Workshops and Demos (ACIIW), pp. 01–08 (2021). <https://doi.org/10.1109/ACIIW52867.2021.9666356>
- [41] Bermejo Nievas, E., Deniz Suarez, O., Bueno García, G., Sukthankar, R.: Violence detection in video using computer vision techniques. In: Computer Analysis of Images and Patterns: 14th International Conference, CAIP 2011, Seville, Spain, August 29-31, 2011, Proceedings, Part II 14, pp. 332–339 (2011). Springer
- [42] Bai, W., Chen, P., Cai, H., Zhang, Q., Su, Z., Cheung, T., Jackson, T., Sha, S., Xiang, Y.-T.: Worldwide prevalence of mild cognitive impairment among community dwellers aged 50 years and older: a meta-analysis and systematic review of epidemiology studies. *Age and ageing* **51**(8), 173 (2022)
- [43] Chen, P., Cai, H., Bai, W., Su, Z., Tang, Y.-L., Ungvari, G.S., Ng, C.H., Zhang, Q., Xiang, Y.-T.: Global prevalence of mild cognitive impairment among older adults living in nursing homes: a meta-analysis and systematic review of epidemiological surveys. *Translational Psychiatry* **13**(1), 88 (2023)
- [44] Chen, L., Dodge, H.H., Asgari, M.: Topic-based measures of conversation for detecting mild cognitive impairment. In: Proceedings of the Conference. Association for Computational Linguistics. Meeting, vol. 2020, p. 63 (2020). NIH Public Access
- [45] Liu, G., Xue, Z., Zhan, L., Dodge, H.H., Zhou, J.: Detection of mild cognitive impairment from language markers with crossmodal augmentation. In: PACIFIC SYMPOSIUM ON BIOCOMPUTING 2023: Kohala Coast, Hawaii, USA, 3–7 January 2023, pp. 7–18 (2022). World Scientific

- [46] Islam, Z., Rukonuzzaman, M., Ahmed, R., Kabir, M.H., Farazi, M.: Efficient two-stream network for violence detection using separable convolutional lstm. In: 2021 International Joint Conference on Neural Networks (IJCNN), pp. 1–8 (2021). IEEE
- [47] Eitta, A.A., Barghash, T., Nafea, Y., Gomaa, W.: Automatic detection of violence in video scenes. In: 2021 International Joint Conference on Neural Networks (IJCNN), pp. 1–8 (2021). IEEE
- [48] Serrano, I., Deniz, O., Espinosa-Aranda, J.L., Bueno, G.: Fight recognition in video using hough forests and 2d convolutional neural network. *IEEE Transactions on Image Processing* **27**(10), 4787–4797 (2018)
- [49] Irfanullah, Hussain, T., Iqbal, A., Yang, B., Hussain, A.: Real time violence detection in surveillance videos using convolutional neural networks. *Multimedia Tools and Applications* **81**(26), 38151–38173 (2022)
- [50] Sernani, P., Falcionelli, N., Tomassini, S., Contardo, P., Dragoni, A.F.: Deep learning for automatic violence detection: Tests on the airtlab dataset. *IEEE Access* **9**, 160580–160595 (2021)
- [51] Ullah, F.U.M., Obaidat, M.S., Muhammad, K., Ullah, A., Baik, S.W., Cuzzolin, F., Rodrigues, J.J., Albuquerque, V.H.C.: An intelligent system for complex violence pattern analysis and detection. *International Journal of Intelligent Systems* **37**(12), 10400–10422 (2022)
- [52] Hanson, A., Pnvr, K., Krishnagopal, S., Davis, L.: Bidirectional convolutional lstm for the detection of violence in videos. In: *Proceedings of the European Conference on Computer Vision (ECCV) Workshops*, pp. 0–0 (2018)
- [53] Li, J., Jiang, X., Sun, T., Xu, K.: Efficient violence detection using 3d convolutional neural networks. In: 2019 16th IEEE International Conference on Advanced Video and Signal Based Surveillance (AVSS), pp. 1–8 (2019). IEEE